

Todo list

Hier fehlt jeweils ein kurzer satz was die dinger bewirken sollen.	2
warum?	3
type	4
eher nur vermutung	8

Contents

Table of Contents	i
List of Tables	i
1 Quality of Nanodiamonds	1
1.1 Quality-improving Post-Processing Treatments	2
1.1.1 Annealing and Oxidation	2
1.1.2 Surface Treatment With Gas And Plasma	3
1.2 Raman Measurements	4
1.2.1 Surface Contamination	5
1.2.2 Defect Concentration	5
1.2.3 Lattice Strain	6
1.3 Transmission Electron Spectroscopy Measurements	8
1.3.1 Crystallinity and Grain Boundaries	8
Bibliography	9

List of Tables

Chapter 1

Quality of Nanodiamonds

Remark:

Ich hab das kapitel jetzt nochmal ueberarbeitet indem ich den aufbau vom SiV papier hier uebernommen hab. Das gibt nochmal einen besseren ueberblick. Es gibt aber noch loecher die du nochmal dezidiert stopfen solltest. Besonders die section mit den post-processing methoden ist noch nicht auf dem niveau der anderen sections in dem kapitel.

- In der introduction werden qualitaetsprobleme genannt und ein paar methoden die da helfen sollen. Hier muss noch kurz erwähnt werden warum die methoden helfen.
- In der ersten section sind annealing und oxidation zusammen. Im text steht aber nur was annealing oder? Falls oxidation dann erst in der naechsten section kommt, sollte man die ueberschriften aendern. Ich kenn mich halt nicht aus, d.h. das passt noch nicht. Es muss auch klar werden welche probleme diese methoden potentiell loesen und warum.
- Was die surface treatments bewirken sollen bzw. wie die die qualitaetsprobleme minimieren? Da ist auch von shells die rede und ich hab keine ahnung was das fuer dinger sind. Hier fehlt auch noch was.
- Wenns um TEM messungen geht, dann ist hier auch von nanodiamond boundaries die rede. Hier sollte jetzt auch eine diskussion boundaries einfließen, bzw. was fuer negative effekte die haben koennen.

Carbon forms a great variety of crystalline and disordered structures because it is able to exist in three hybridisations, sp^3 , sp^2 , $sp^1(??)$ [4]. In the sp^3 configuration, as in diamond, a carbon atom's four valence electrons are each assigned to a tetrahedrally directed sp^3 orbital, which makes a strong σ bond to an adjacent atom. In the three-fold coordinated sp^2 configuration as in graphite, three of the four valence electrons enter trigonally directed sp^2 orbitals, which form σ bonds in a plane. The fourth electron of the sp^2 atom lies in a $p_z(p\pi)$ orbital, which lies normal to the σ bonding plane. This π

orbital forms a weaker π bond with an π orbital on one or more neighbouring atoms. In the sp^1 configuration, two of the four valence electrons enter σ orbitals, each forming a σ bond directed along the $\pm x$ -axis, and the other two electrons enter $p\pi$ orbitals in the y and z directions. The extreme physical properties of diamond derive from its strong, directional σ bonds. Graphite has strong intra-layer σ bonding and weak van der Waals bonding between its layers [5].

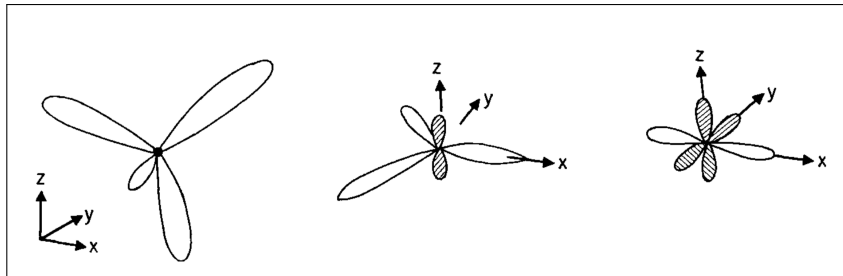


Figure 1.1: The sp^3 , sp^2 , sp^1 hybridised bonding [4]

In this thesis we perform measurements of SiV centers hosted in nanodiamonds produced by various means ???. In this context we use the term quality as a measure of how close diamond crystals are to their pristine form. The presence of lattice imperfections such as additional vacancies, lattice strain, impurities or the inclusion of graphite or amorphous carbon is known to adversely affect crystal quality [1, 2, 3].

Surface contamination like graphite and amorphous sp^2 hybridized carbon atoms manifest themselves as additional peaks in the Raman spectrum. Strain in the diamond lattice broadens the first order Raman peak and causes it to shift to higher or smaller wavenumbers. Similarly, high concentrations of lattice defects cause additional peaks, a broadening of the first order Raman peak and a shift towards smaller wavenumbers. To improve crystal quality and to reduce the mentioned distracting effects the following methods are deployed here: Annealing in a vacuum, oxidation in air as well as surface treatments involving plasmas.

To study the effectiveness of these treatments and to gauge the quality of our nanodiamond samples we rely on Raman spectroscopy and TEM imaging. The former is used to detect strain, quantify defect concentration and the presence of carbon in non-diamond phases, while the latter enables imaging of individual nanodiamonds revealing details in crystallinity such as crystal boundaries.

1.1 Quality-improving Post-Processing Treatments

1.1.1 Annealing and Oxidation

In this thesis we perform measurements with nanodiamonds produced both by direct CVD growth and by wet-milling a CVD diamond film. In a chemical vapor deposition reactor, either an amorphous carbon deposit, or a crystalline diamond film may be

produced depending on the ratio of the fluxes of carbon and atomic hydrogen onto a substrate [6, 7].

SiV centers were formed both via *in-situ* implantation during CVD growth and via silicon implantation. During silicon implantation the diamond lattice gets damaged by the penetrating ions. sp^2 bonds, carbon interstitials and vacancies disrupt the metastable equilibrium of the diamond phase. Hence, there is a tendency for damaged diamond to "tip over" to the thermodynamically stable form of carbon, i.e. graphite.

At temperatures above about 500 °C, vacancies in the diamond lattice become mobile and diffuse towards the surface[8]. Literature suggests, that annealing at 900 °C for 1 h is sufficient to remove most of the damage following implantations. To reduce the damage in the diamond lattice even further, we anneal the implanted diamonds at 900 °C to 1200 °C for 3 h to 6 h in vacuum (10^{-6} Pa).

The surface of the nanodiamonds is contaminated with graphite and amorphous sp^2 hybridized carbon . We apply oxidation in an oven under ambient air at a temperature of 450 °C for 3 h to 6 h.

warum?

1.1.2 Surface Treatment With Gas And Plasma

We wanted to assert whether surface treatments with different gases influence the emission properties, so we treated them with hydrogen (H_2), oxygen (O_2), ozone (O_3) all both at room temperature and at 500 °C; and also with H_2 plasma. However, we found that most nanodiamonds treated in this way only showed luminescence which immediately bleached when illuminated with a cw 660 nm laser even at low excitation powers of 200 μ W, or no luminescence at all. We double-checked with a CCD-image of the surface to be sure that there are nanodiamonds in the focus. This bleaching occurred so quickly, that after a scanning no spectrum could be taken. The only samples which did yield spectra with measurable ZPLs were the ones treated with H_2 . However, also these SiV centers were not single ones. Therefore, we did not further investigate these samples.

One sample showed shells around the nanodiamond after oxidizing in air. We attribute this effect to a contamination in the oven. When we illuminated these nanodiamonds in the SEM for several moments, the shell went away. We therefore deducted that the shell is organic material. To get rid of the shells on the whole sample, we treated it with oxygen-argon plasma for 3 min¹. After the first treatment, the shells were smaller, but not gone. So we put them into the oxygen-argon plasma again for 3 min, however, the shells were bigger than before any treatment. We tried another approach to get rid of the shells with ozone treatment for 4 h at 360 °C. Before ozone treatment there the diamond Raman line and other Raman lines visible. After surface treatment, more lines appeared and all of these other lines got more intense. There are probably organic contaminations on the sample in which functional groups got introduced by the ozone treatment. We did not further investigate this sample and defined it as broken.

¹Treatment performed by J. Schmauch, group of R. Birringer, Saarland University

1.2 Raman Measurements

Raman spectroscopy of various samples gives insight into crystal quality and surface contamination of nanodiamonds. Raman scattering is the inelastic scattering of a photon $\hbar\omega_i$ on a molecule or crystal lattice in the initial state $|i\rangle$ with energy E_i . The molecule or crystal transitions into a higher energy state E_f and the scattered photon with frequency ω_s loses the energy $\Delta E = E_f - E_i = \hbar(\omega_i - \omega_s)$. Therefore, energy is exchanged between the photon and the excited matter, changing the rotational or oscillation energy of the involved molecule or the oscillation energy, i.e. phonons of the crystal lattice. The Raman shift is typically referenced in wavenumbers. It is given by:

$$\Delta\omega = \left(\frac{1}{\lambda_{ex}} - \frac{1}{\lambda_R} \right) \quad (1.1)$$

As every solid exhibits characteristic phonon modes tied to the properties of its lattice structure, Raman spectroscopy can be used to characterize diamond. Raman measurements of wet-milled nanodiamonds give insight into the issues of surface contamination, lattice strain and defect concentration: Surface contamination like graphite and amorphous sp² hybridized carbon atoms cause additional peaks in the Raman spectrum. A high defect concentration may lead to additional peaks, a broadening of the first order Raman peak and a shift to smaller wavenumbers. Strain in the diamond broadens the first order Raman peak and causes a shift to higher wavenumbers [1, 2, 3].

For the Raman measurements the same layout of the setup described in ?? is used. As an excitation light source, a 532 nm continuous wave diode laser is used (IO). It provides single frequency mode laser light, a prerequisite for Raman investigations. The beamsplitter is a dichroic mirror (DRLP645), the laser light is additionally filtered out with a 532 Notch filter in the detection path in front of the single mode fiber instead of a long pass filter. With these adaptations, the combination of the confocal unit and the spectrometer serves as a Raman spectrometer. As the diamond Raman line is very narrow, the 600 grooves/mm grating is used to as a starting point. Detailed measurements are realized using 1200 grooves/mm and 1800 grooves/mm gratings.

Since the size of single nanodiamonds is on the order of tens of nanometers, low signal intensities can become an issue when taking Raman measurements. To overcome this problem we pursue two different approaches:

- a) Nanodiamond Clusters: Collective measurements are carried out at several areas on the sample insitu70. Since this sample is densely covered with nanodiamonds, collective measurements of clusters of nanodiamonds (??) achieves higher signal intensities.
- b) Big Nanodiamonds: Raman measurements are carried out on the implanted sample implanted250ao. For this sample, diamond particles are big enough to yield sufficient intensities on single nanodiamonds.

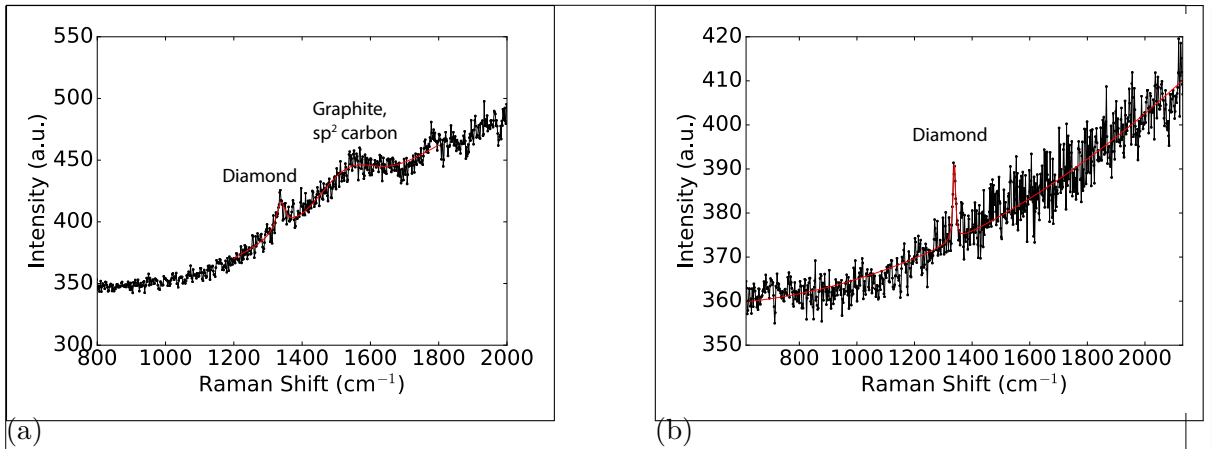


Figure 1.2: Raman measurements, black: data, red: fit. (a) Raman measurement before oxidation, sample insitu70. The diamond Raman peak is situated at 1338 cm^{-1} . The broad feature around 1580 cm^{-1} corresponds to the graphite G-band. (b) Raman measurement after oxidation, sample insitu70o. The G-band has vanished, indicating removal of graphite and amorphous sp^2 hybridized carbon.

1.2.1 Surface Contamination

We test the impact of oxidation treatment as described in ?? on surface contamination. ?? shows a measured Raman spectrum of a sample without oxidation treatment (insitu70n). To verify reproducibility, the measurement is performed on three different spots of the sample. The narrow peak in ?? corresponds to the first order diamond Raman peak and will be further analyzed in ?? . The spectrum also shows a broad peak with a Raman shift of about $(1582 \pm 5)\text{ cm}^{-1}$. This shift corresponds to the G-band due to amorphous sp^2 hybridized carbon atoms and graphite. The exact G-band position and linewidth is sensitive to parameters such as the clustering of the sp^2 phase, bond-length and bond-angle disorder, presence of sp^2 rings or chains, and the sp^2/sp^3 ratio [9]. The nanodiamond Raman spectra are considerably modified after oxidation in air at $450\text{ }^\circ\text{C}$. To verify this, we perform Raman measurements on three different spots of a sample produced in the same process as the above mentioned, which is additionally oxidized (insitu70o). While the G-band peak is present in every measurement performed on a non-oxidized sample, it is not present in any of the oxidized samples (??), indicating successful removal of sp^2 hybridized carbon and surface graphite.

1.2.2 Defect Concentration

Several effects impact the first order diamond Raman line: 1. defects in the diamond lattice, 2. hydrostatic pressure, 3. uniaxial or more complicated stress configurations. In the measurement on nanodiamond clusters the width of the diamond Raman peak of sample insitu70 varies between 15 cm^{-1} and 30 cm^{-1} without oxidation treatment, but is only 9 cm^{-1} to 11 cm^{-1} after the oxidation process. A possible reason for this change of

the width is improved crystal quality [2]. In the measurement on big nanodiamonds we measured a Raman line at $(1308 \pm 5) \text{ cm}^{-1}$ (denoted line R1) which exhibits a broad linewidth of $(25 \pm 5) \text{ cm}^{-1}$. One plausible explanation for both the position and the linewidth of the Raman line are defects in the diamond lattice[2].

1.2.3 Lattice Strain

We investigated how strain in the diamond lattice manifests itself in both measurements on nanodiamond clusters and on big nanodiamonds. In the Raman measurement on nanodiamond clusters, the position of the diamond Raman peak is the same for oxidized (insitu70o) and non-oxidized (insitu70n) samples, indicating that oxidation does not affect strain in the diamond. However, the Raman shift of both non-oxidized and oxidized samples amounts to $(1338 \pm 5) \text{ cm}^{-1}$, as compared to the literature value of 1332.5 cm^{-1} of pristine diamond [1] (given uncertainties are governed by spectrometer resolution). This shift indicates the presence of strain in the diamond particles.

Performing the Raman measurement on big nanodiamonds we found one diamond Raman line at $(1308 \pm 5) \text{ cm}^{-1}$ (line R1), one at $(1345 \pm 5) \text{ cm}^{-1}$ (line R2) and one at $(1348 \pm 5) \text{ cm}^{-1}$ (line R3), indicating a broad distribution of strain among the individual diamond particles (uncertainties governed by spectrometer resolution). Only line R1 can be explained with a high defect concentration in the diamond lattice due to its shift to smaller wavelength. However, a more consistent model which explains all occurring shifts is the presence of strain in the diamond nano particles. From the linewidths in the measurement on big nanodiamonds, the strain in the diamond is calculated using the equation for hydrostatic pressure [2]

$$\omega(P) = \omega_0 + a_1 P + a_2 P^2, \quad (1.2)$$

where $\omega_0 = 1332.5 \text{ cm}^{-1}$, $a_1 = 2.83 \text{ cm}^{-1} \text{ GPa}^{-1}$ and $a_2 = -3.65 \times 10^{-3} \text{ cm}^{-1} \text{ GPa}^{-1}$. The calculation yields a pressure in the investigated diamonds of -8.56 GPa tensile stress and 4.26 GPa and 5.50 GPa compressive stress. Pressure uncertainties due to the Raman line measurements are smaller than one Pascal and are therefore neglected. Under hydrostatic pressure, the triply degenerate first order Raman peak remains degenerate, while under uniaxial and more complex stress configurations (biaxial stress, shear stress etc.) mode splitting occurs [2]. As mentioned above, we observe broad linewidths up to $(25 \pm 5) \text{ cm}^{-1}$. The broad linewidths of the Raman lines may be attributed to uniaxial strain, as mode splitting manifests itself in a broadening of the peak due to limited spectrometer resolution. Therefore, we conclude that both hydrostatic and uniaxial strain is present in the nanodiamonds.

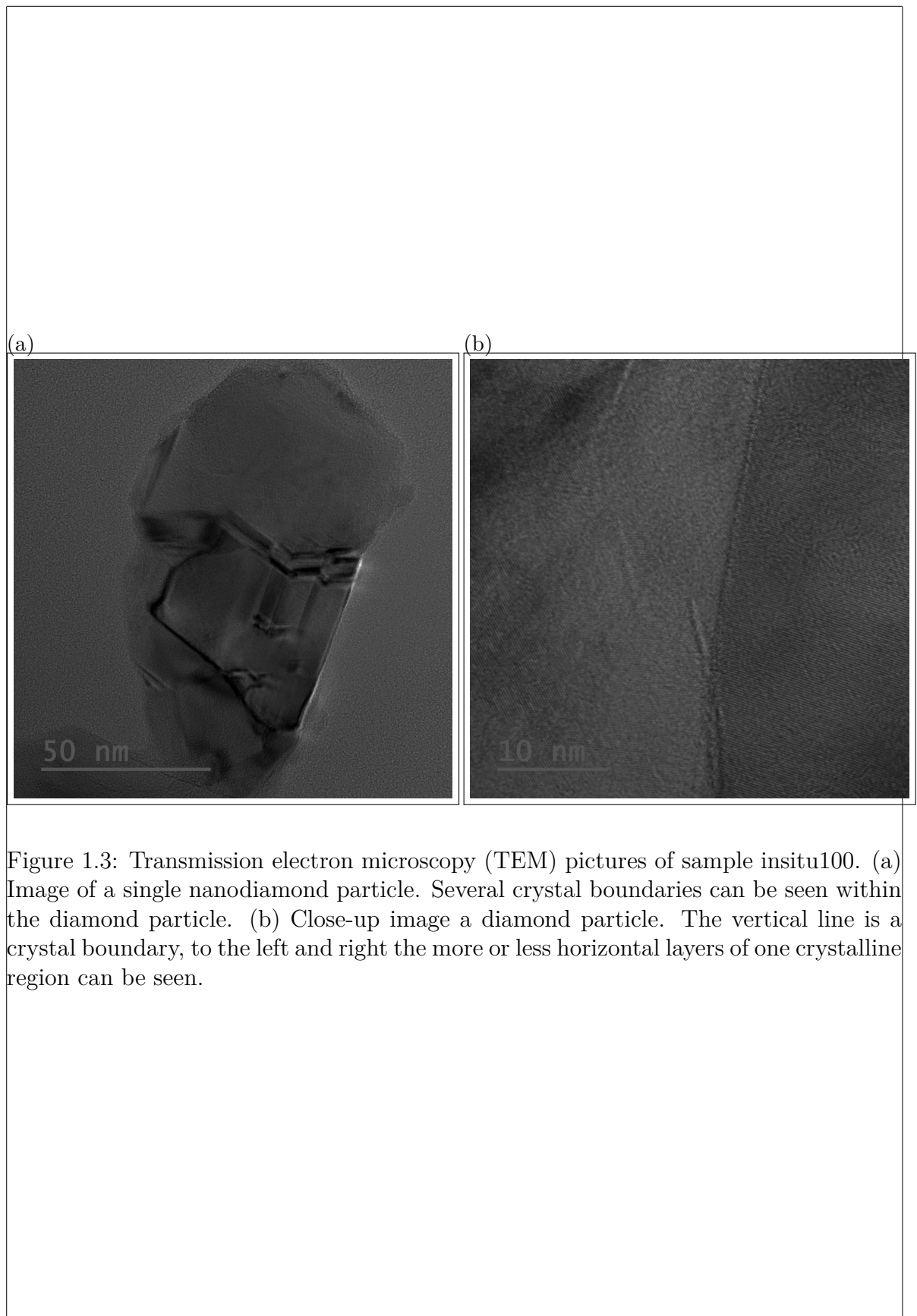


Figure 1.3: Transmission electron microscopy (TEM) pictures of sample insitu100. (a) Image of a single nanodiamond particle. Several crystal boundaries can be seen within the diamond particle. (b) Close-up image a diamond particle. The vertical line is a crystal boundary, to the left and right the more or less horizontal layers of one crystalline region can be seen.

1.3 Transmission Electron Spectroscopy Measurements

Transmission electron microscopy (TEM, also sometimes conventional transmission electron microscopy or CTEM) is a microscopy technique in which a beam of electrons is transmitted through a specimen to form an image. The specimen is most often an ultra-thin section less than 100 nm thick or a suspension on a grid. An image is formed from the interaction of the electrons with the sample as the beam is transmitted through the specimen. During transmission electron microscopy a beam of electrons is transmitted through a sample, forming an image of the transmitted sample. Since electrons have higher de Broglie wavelengths than photons, a higher resolution is obtainable, allowing the surface of nanodiamonds to be resolved. Thus, the crystallinity of single nanodiamonds can be studied directly.

1.3.1 Crystallinity and Grain Boundaries

Sample insitu100 was investigated using TEM by J. Schmauch, group of R. Birringer, Saarland University. Smaller nanodiamonds would have been too small for the carbon grid which serves as a sample holder in the TEM, and might have fallen through the grid and bigger particles would have been too big to be transmitted by the electron beam, making the imaging impossible. In Figure 1.3 there are TEM images, one of them exhibits a single diamond particle and the other is a close-up image of a crystal boundary. From Figure 1.3a it can be seen that the diamond particle contains several crystallites and crystal boundaries. The edges of the crystallites are the sharp features within the diamond particle, the crystal boundaries the smoother features. In Figure 1.3b the crystal layers which are more or less horizontal and in more or less the middle of the picture there is a vertical line which is the edge of a crystallite. So it is clear that the investigated sample does not contain beautiful single crystal diamond particles, which means a reduction of the crystal quality of the diamond particles.

Bibliography

- [1] AM Zaitsev. *Optical properties of diamond: a data handbook*. 2001. 2, 4, 6
- [2] Steven Prawer and Robert J Nemanich. Raman spectroscopy of diamond and doped diamond. *Philosophical Transactions of the Royal Society A: Mathematical, Physical and Engineering Sciences*, 362(1824):2537–2565, nov 2004. 2, 4, 6
- [3] J. O. Orwa, K. W. Nugent, D. N. Jamieson, and S. Prawer. Raman investigation of damage caused by deep ion implantation in diamond. *Physical Review B - Condensed Matter and Materials Physics*, 62(9):5461–5472, sep 2000. 2, 4
- [4] J Robertson. Advances in Physics Amorphous carbon. *Advances in Physics*, 35:317–374, 1986. 1, 2
- [5] J. Robertson. Diamond-like amorphous carbon. *Materials Science and Engineering: R: Reports*, 37(4-6):129–281, may 2002. 2
- [6] Ij Ford. Model of the Competitive Growth of Amorphous-Carbon and Diamond Films. 78(1):510–513, 1995. 3
- [7] Darin S. Olson, Michael A. Kelly, Sanjiv Kapoor, and Stig B. Hagstrom. Sequential deposition of diamond from sputtered carbon and atomic hydrogen. *Journal of Applied Physics*, 74(8):5167–5171, 1993. 3
- [8] M. S. Dresselhaus and R. Kalish. *Ion Implantation in Diamond, Graphite and Related Materials*, volume 22 of *Springer Series in Materials Science*. Springer Berlin Heidelberg, Berlin, Heidelberg, 1992. 3
- [9] Andrea Carlo Ferrari and John Robertson. Raman spectroscopy of amorphous, nanostructured, diamondâ€¢like carbon, and nanodiamond. *Philosophical Transactions of the Royal Society of London A: Mathematical, Physical and Engineering Sciences*, 362(1824):2477–2512, 2004. 5